J. Fluid Mech. (1996), *vol.* 308, *pp.* 15–29

Surface manifestations of turbulent flow

By MICHAEL S. LONGUET-HIGGINS
Institute for Nonlinear Science, University of California, San Diego, La Jolla, CA 92093-0402, USA

(Received 30 May 1995 and in revised form 21 August 1995)

The surface of a turbulent, open-channel flow is often characterized by smooth areas of upwelling, each surrounded by a zone of downwelling marked by short steep waves. The dynamics of short waves on such a downwelling region are investigated and some laboratory experiments are proposed. Assuming that the horizontal strain rate Ω is locally constant, a simple expression is derived for the amplitude a of the short capillary–gravity waves, and hence also for the spectrum of the surface slopes.

1. Introduction

The flow in rivers and tidal channels, as well as in ships' wakes, is usually turbulent, and the most immediate way of detecting subsurface eddies is by the effects that they produce at the upper surface of the fluid. The question arises: what is the nature of the surface indications that we can detect by eye or by other kinds of remote sensing? Further, what can we infer from such observations concerning the nature of the subsurface flow?

These questions were prompted by a visit which the author made to the Skookumchuck Narrows in British Columbia in order to see the strong tidal current there, which at spring tides attains a speed of about 20 km h^{-1} (5.6 m s^{-1}); see King (1956). A video picture of the flow is reproduced in figure 1.† One feature frequently observed was the occurrence of a broad patch of relatively smooth water spreading outwards from a line, or a centre, of upwelling. Near the middle of this smooth patch there often appeared a secondary upwelling, whose boundaries were marked by a ring of short capillary waves, as in figure 2. The area of the secondary upwelling gradually grew and sometimes a daisy-chain of small vortices could be seen around the boundary. This suggested the breakup of a vortex sheet, as if the fluid in the secondary upwelling was rotating relative to the first. Meanwhile the whole pattern was convected downstream.

In answer to the first question above, it appears that the surface indications of the flow are of two kinds: short capillary waves, which are visible through their relatively steep slopes; and vortices, which by centrifugal force produce small circular indentations.

The observed patterns just described have been attributed by Allen (1985) to 'kolks' beneath the surface, as described by Mathes (1947). These are organized turbulent structures generated at the lower boundary of the flow. The surface patterns themselves are referred to as 'kolk boils' (see Nezu & Nakagawa 1993).

The purpose of the present paper, which was stimulated by these observations, is to

† A similar though less striking photograph of a tidal current in the Severn Estuary is shown in figure 9.1 of Nezu & Nakagawa (1993).

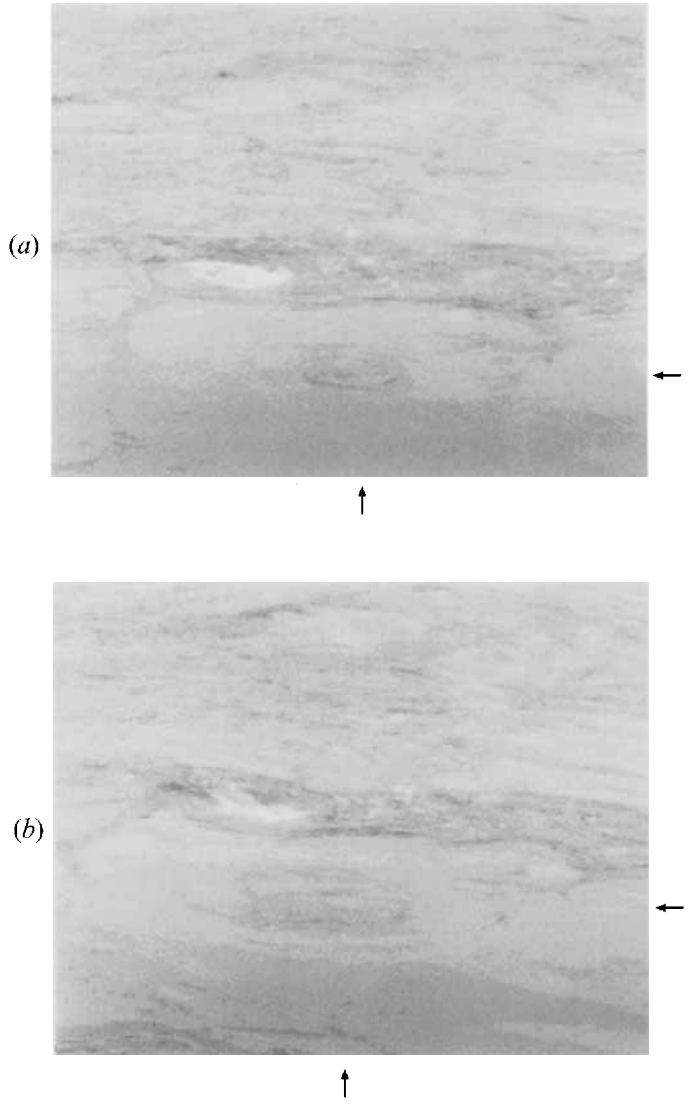

FIGURE 1. View of the tidal current in the Skookumchuck Narrows, showing the growth of an upwelling zone (indicated by arrows) in a larger smooth area, at two successive instants.

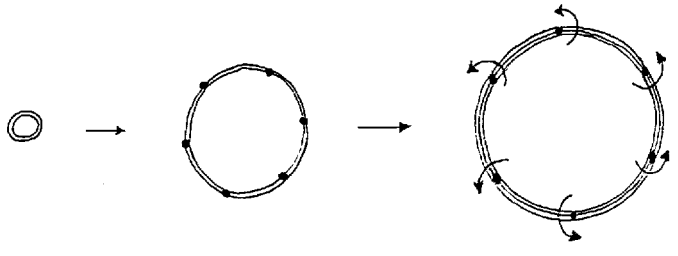

FIGURE 2. Schematic of ripples and eddies at the edge of an upwelling zone.

determine the analytic form of the ripples seen at the boundary of an upwelling zone. We begin in §2 with a discussion of the dynamics of short waves on a non-uniform current, a topic considered previously by Longuet-Higgins & Stewart (1964), Bretherton & Garrett (1968), Shyu & Phillips (1990) and most recently Trulsen & Mei (1993). For two-dimensional waves we derive the simple equation (2.12) governing the action density A. Here $U(x)$ denotes the current at the surface, c_g is the group velocity and ν the kinematic viscosity. In §3 we see that if the strain rate $\partial U/\partial x$ is locally constant, then the action density A is given by a very simple expression. In §4 we describe the kinematics of the wave pattern, including the phenomenon of double reflection also discovered by Trulsen & Mei (1993). Some special cases, with possible experimental tests, are treated in §§5–8. In §8 we derive a time-dependent solution. Lastly in §9 we point out that from the expression for the action density we can infer a form for the spectral density $S(k)$ of the surface slope which while depending on the strain rate Ω is independent of the parameter σ_0 (the radian frequency of the waves relative to a stationary observer). This expression may be of use in estimating the radar backscatter from a turbulent current, or inferring the scale of the turbulence from measurements of the backscatter.

2. Basic equations

Consider a train of surface waves of local amplitude a and wavenumber k riding on a steady, non-uniform current of speed U, as shown in figure 3. The current is positive to the right; the waves travel with speed c to the right. The current is assumed to vary gradually in the x-direction, in the sense that $\partial U/\partial x \ll \sigma$ where σ is the radian frequency of the waves, relative to an observer moving with speed U. We shall suppose that σ is given by the dispersion relation for inviscid, or weakly damped, capillary–gravity waves, namely

$$\sigma^2 = gk + (T/\rho)k^3, \tag{2.1}$$

where g, T and ρ denote gravity, surface tension and density respectively. It will be convenient to choose units so that

$$g = T = \rho = 1. \tag{2.2}$$

First we consider quasi-steady conditions in which a, k and σ are independent of the time t. Then we have two basic conservation equations: (i) the conservation of phase, given by

$$\sigma + kU = k(U+c) = \sigma_0, \quad \text{constant}, \tag{2.3}$$

where $c = \sigma/k$, the local phase speed, and (ii) the conservation of energy, given by

$$\frac{\partial}{\partial x}[E(U+c_g)] + S_{xx}\frac{\partial U}{\partial x} + 4\nu k^2 E = 0 \tag{2.4}$$

(see for example Longuet-Higgins & Stewart 1964). Here E denotes the local energy density of the waves:

$$E = \tfrac{1}{2}a^2(1+k^2), \tag{2.5}$$

c_g denotes the group velocity $\mathrm{d}\sigma/\mathrm{d}k$, given by

$$c_g = \frac{(1+3k^2)}{2(1+k^2)}c, \tag{2.6}$$

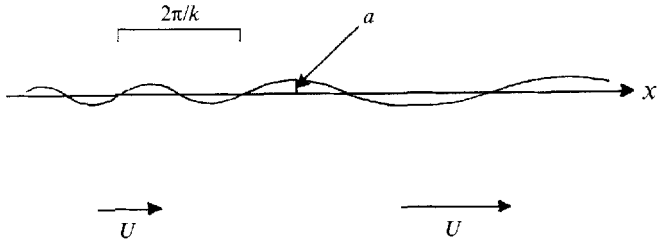

FIGURE 3. Waves on a non-uniform current U.

and S_{xx} is the radiation stress, given by

$$S_{xx} = \tfrac{1}{2}E\frac{1+3k^2}{1+k^2} = E\frac{c_g}{c}. \tag{2.7}$$

The last term on the left of (2.4) represents the internal viscous dissipation (see Lamb 1932, p. 624), ν being the kinematic viscosity. It is assumed that the waves are in relatively deep water. Equation (2.4) can be rewritten in terms of the action density

$$A = E/\sigma. \tag{2.8}$$

On multiplying each side by $1/\sigma$ equation (2.4) becomes

$$\left\{\frac{\partial}{\partial x}\left[\frac{E(U+c_g)}{\sigma}\right] - E(U+c_g)\frac{\partial}{\partial x}\left(\frac{1}{\sigma}\right)\right\} + E\frac{c_g}{\sigma c}\frac{\partial U}{\partial x} + 4\nu k^2 E/\sigma = 0. \tag{2.9}$$

But

$$\frac{\partial}{\partial x}\left(\frac{1}{\sigma}\right) = -\frac{1}{\sigma^2}\frac{\partial \sigma}{\partial x} = -\frac{1}{\sigma^2}c_g\frac{\partial k}{\partial x}, \tag{2.10}$$

since $c_g = \mathrm{d}\sigma/\mathrm{d}k$. By differentiating (2.3) we find also

$$(U+c_g)\frac{\partial k}{\partial x} + k\frac{\partial U}{\partial x} = 0. \tag{2.11}$$

Hence the second and third terms in (2.9) cancel and we have simply

$$\frac{\partial}{\partial x}[A(U+c_g)] + 4\nu k^2 A = 0, \tag{2.12}$$

see Shyu & Phillips (1990).

The original version of (2.12) (Garrett 1967; Bretherton & Garrett 1968) did not include the dissipation term. We have derived (2.12) in this way to show how it follows from the more familiar energy equation. Shyu & Phillips (1990) give a slightly longer proof.

3. Solution of equation (2.12): uniform strain rate

In general we can write

$$A(U+c_g) = B, \tag{3.1}$$

representing the action *flux*. Then (2.12) becomes

$$\frac{\partial B}{\partial x} = -\frac{4\nu k^2}{U+c_g}B \tag{3.2}$$

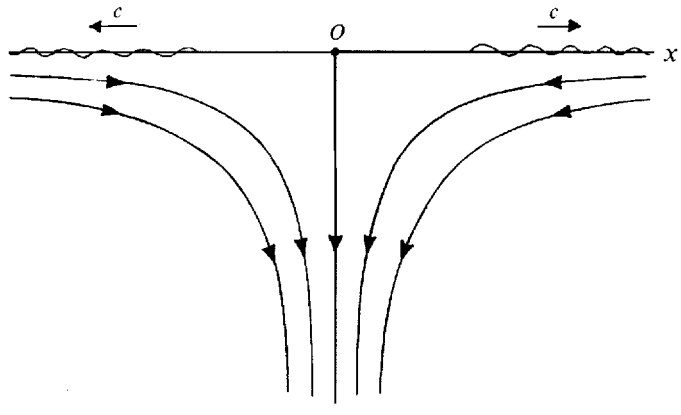

FIGURE 4. Flow in the neighbourhood of a convergence.

whence on integration

$$B = \exp\left[-\int \frac{4\nu k^2}{U+c_g}\,\mathrm{d}x\right]. \tag{3.3}$$

But from (2.11) we have

$$\frac{\mathrm{d}x}{U+c_g} = -\frac{\mathrm{d}k}{k\,\partial U/\partial x}. \tag{3.4}$$

Therefore (3.3) becomes

$$B = \exp\left[\int \frac{4\nu k}{\partial U/\partial x}\,\mathrm{d}k\right]. \tag{3.5}$$

Now in the neighbourhood of a stagnation point, where there is a convergence of the surface current (see figure 4) we may write

$$U = -\Omega x, \quad \frac{\partial U}{\partial x} = -\Omega, \tag{3.6}$$

where Ω is a positive constant. Then (3.5) becomes

$$B = B_0 \mathrm{e}^{-2\nu k^2/\Omega}, \tag{3.7}$$

where B_0 is an arbitrary constant. Hence

$$A = \frac{B_0}{U+c_g}\mathrm{e}^{-2\nu k^2/\Omega} \tag{3.8}$$

and

$$E = \frac{B_0\,\sigma}{U+c_g}\mathrm{e}^{-2\nu k^2/\Omega}. \tag{3.9}$$

The wave amplitude a is then found from (2.5) to be

$$a = \left(\frac{2E}{1+k^2}\right)^{1/2}. \tag{3.10}$$

4. Nature of the solution

With the assumption of a linear strain rate, the equation of phase conservation (2.3) becomes

$$\sigma = \sigma_0 + \Omega x k. \tag{4.1}$$

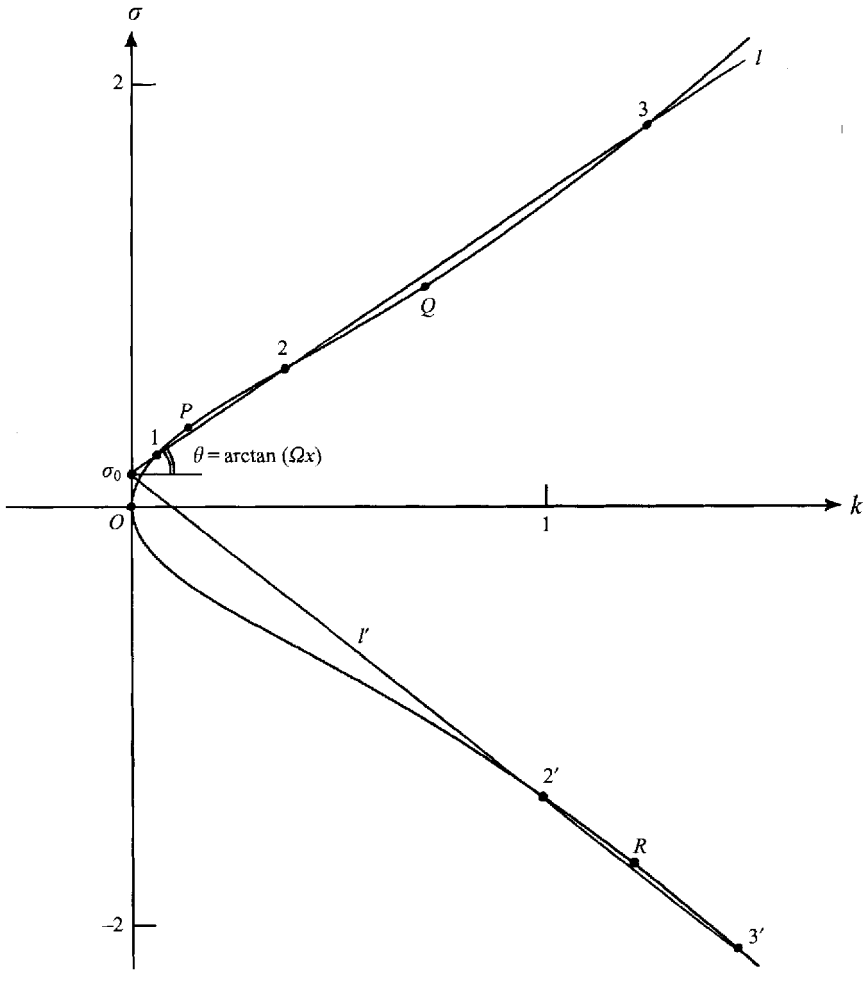

FIGURE 5. Diagram for obtaining the roots of equation (4.3) in the (k, σ)-plane.

Combining this with the dispersion relation

$$\sigma^2 = k + k^3 \tag{4.2}$$

we obtain a cubic equation

$$k^3 + k = (\Omega x k + \sigma_0)^2 \tag{4.3}$$

to solve for k as a function of x. This has in general either one real root or three. Exceptionally, two of the roots may coincide, or possibly all three; compare for example Basovich & Talanov (1977), Shyu & Phillips (1990), Trulsen & Mei (1993).

Figure 5 shows the situation in the (k, σ)-plane. By (4.2) the wavenumber k is non-negative. For given x, (4.1) represents a straight line l in the (k, σ)-plane, passing through the fixed point $(0, \sigma_0)$ on the σ-axis and making an angle $\theta = \arctan(\Omega x)$ with the k-axis. This meets the dispersion curve (4.2) at either one or three points, generally, depending on the values of σ_0 and θ (or x).

Suppose first that σ_0 and x are positive. Let the tangent to the dispersion curve at the point of inflexion I meet the σ-axis in the point $(0, \sigma_c)$, say. If $0 < \sigma_0 < \sigma_c$, and $x > 0$, then the line l meets the dispersion curve at three distinct points (1), (2), (3) but only if θ lies in a certain range bounded by the tangents at P and Q. If l passes through P, say, then the two roots (1) and (2) coincide at P, and if l passes through Q the roots (2) and (3) coincide at Q.

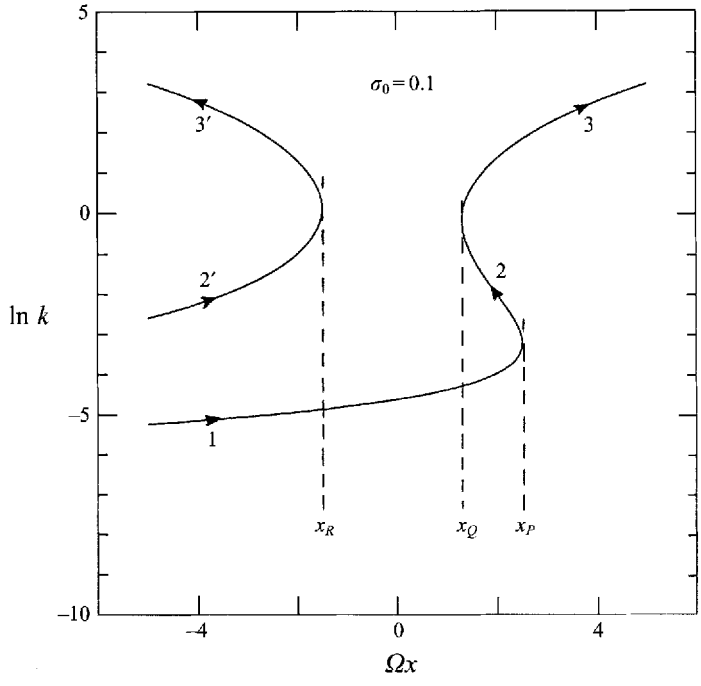

FIGURE 6. Diagram of the wave system in the (x,k)-plane corresponding to figure 5, when $\sigma_0 = 0.1$. The wave systems (1), (2), (3) correspond to the intersections (1), (2), (3) in figure 5. Arrows denote the direction of action flux.

When $\sigma_0 = \sigma_c$, then P and Q come to I, and all three roots also coincide at I. On the other hand if x and 0 are negative, there are either three roots of (4.3) or one, according as l lies inside or outside a sector bounded by the tangents at R and O (the latter is the negative σ-axis).

The situation in the (x,k)-plane is shown diagrammatically in figure 6. The points x_P, x_Q, x_R on the x-axis correspond to P, Q and R of figure 5. When $x > x_P$ there is only one wave system (3). This is a strongly capillary wave, with high wavenumber k. The flux of energy $E(U+c_g)$ is positive, since c_g, which is given by the gradient of the tangent to the dispersion curve, is greater than Ωx, the gradient of the line l.

When $x_Q < x < x_P$ there are three distinct systems of waves. In (1) and (3) the flux is positive, and in (2) it is negative. When $x_R < x < x_Q$ there is only one wave system namely (1), with small wavenumber k. It is a gravity-type wave and the flux is positive.

When $x < x_R$ two other wave systems appear which we call (2)′ and (3)′. The action fluxes are negative and positive respectively. These systems are disconnected energetically from system (1).

Each of the critical points x_P, x_Q and x_R is clearly a caustic, at which two distinct wave systems fuse. In the neighbourhood of such points $(U+c_g)$ is small, making both A and E large, in our approximation. However, a higher-order theory such as was used by Smith (1975) is then applicable. In this the wave amplitudes are locally described by Airy functions, and remain finite.

It is clear that as σ_0 approaches σ_c from below, the two points x_P and x_Q come together to form a higher-order singularity. The wave system (2) is then extinguished. Thirdly when $\sigma_0 > \sigma_c$ the wave system (3) merges continuously into (1) without any singularity. However, the caustic at x_R remains.

σ_0	f (Hz)	Ωx_R	Ωx_Q	Ωx_P
0.0	0.000	−1.41	1.41	∞
0.1	0.948	−1.51	1.31	2.50
0.2	1.896	−1.59	1.17	1.28
0.2467	2.339	−1.63	1.09	1.09
0.3	2.844	−1.67	—	—
0.5	4.740	−1.80	—	—
0.7	6.636	−1.92	—	—
1.0	9.480	−2.08	—	—

TABLE 1. Representative frequencies and velocities

We have so far supposed $\sigma_0 > 0$, with x or θ either positive or negative. If $\sigma_0 < 0$, the discussion proceeds in a precisely similar way by symmetry, since the dispersion curve is its own reflection in the σ-axis.

Note that our figure 6 is similar to figure 4 of Trulsen & Mei (1993), except that they did not include the curves corresponding to negative frequencies. In c.g.s. units in which $g = 981$ and $T = 75$, the frequency f (in Hz) corresponding to a dimensionless radian frequency σ_0 is given by

$$f = \left(\frac{g^3}{T}\right)^{1/4} \frac{\sigma_0}{2\pi} = 9.480\sigma_0. \tag{4.4}$$

For convenience, some representative values are given in table 1.

5. The special case $\sigma_0 = 0$

Two special cases are of interest. The first is when $\sigma_0 = 0$, that is, the frequency $k(U+c)$ relative to a stationary observer is zero, so that the wave pattern is stationary. The situation in the (k, σ)-plane is shown in figure 7. The figure is symmetric with respect to θ or σ. Hence in the (x, k)-plane (figure 8) we have symmetry about $x = 0$. Since P tends to O in figure 7, OP becomes vertical and so in figure 8, x_P tends to infinity. Equation (4.3) has one root $k = 0$ which we may ignore, along with wave system (1). The remaining two roots of (4.3) are given by

$$k^2 - (\Omega x)^2 k + 1 = 0. \tag{5.1}$$

Hence

$$k = \tfrac{1}{2}(\Omega x)^2 \pm [\tfrac{1}{4}(\Omega x)^4 - 1]^{1/2}. \tag{5.2}$$

The roots are real only if

$$\tfrac{1}{4}(\Omega x)^4 \geqslant 1 \tag{5.3}$$

so there are two caustics given by

$$x = \pm\sqrt{2}/\Omega \tag{5.4}$$

or in dimensional units

$$x = \pm(4gT)^{1/4}/\Omega. \tag{5.5}$$

In figure 7 these correspond to the two tangents l from O to the curve at Q and R, which correspond to minima of the phase speed $|c|$.

In other words there is a calm patch in the central zone of figure 8. Outside this zone there are two systems of waves: (2) and (3) on the right and (2)′ and (3)′ on the left. On each side, the action flux outwards in the capillary-type wave exactly balances the flux inwards from the gravity-type wave, apart from viscous damping. Because the

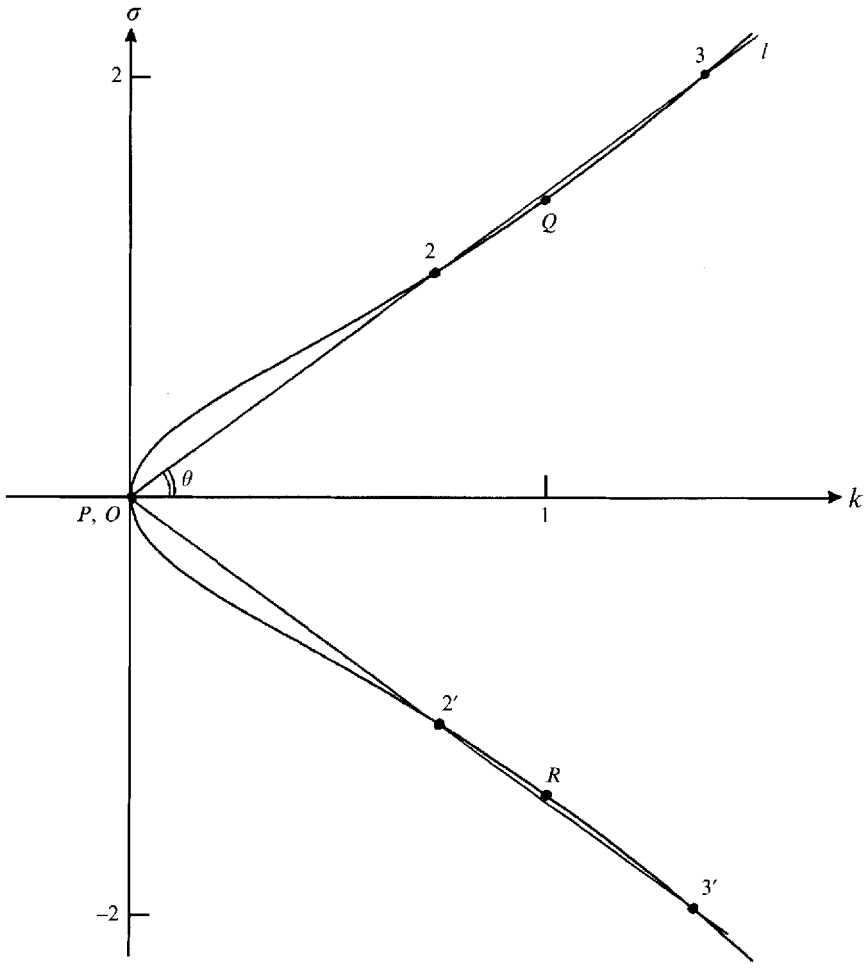

FIGURE 7. Situation in the (k, σ)-plane when $\sigma_0 = 0$.

waves in the calm zone $|x| < \sqrt{2}\Omega^{-1}$ are vanishingly small (Ω being small, by assumption) the two systems of waves, on the left and on the right respectively, are effectively decoupled and independent of one another; one system may exist in the absence of the other.

In practice the above picture may have to be modified. For, since the wave amplitude is greatest at a caustic, wave breaking will most likely occur there, resulting in a loss of energy and of wave action. However, if the incoming gravity wave is of very low amplitude it may not break, or may break only partially. Being of low amplitude and relatively large wavelength it will have a very low steepness and so may be hardly visible to the eye, whereas the 'reflected' capillary wave will be much steeper, and hence may be clearly visible. The capillary wave will therefore appear to 'spring out of nothing' at a point slightly beyond the wave caustic, i.e. $x = \sqrt{2}/\Omega + \epsilon$, $\epsilon > 0$. In fact such a phenomenon may be expected for all values of σ_0 in the range $0 < \sigma_0 \leqslant \sigma_c$.

6. Experimental tests

In a flume of running water, let a vertical plane barrier be inserted through the surface to a depth H, as in figure 9. The water velocity before insertion of the barrier

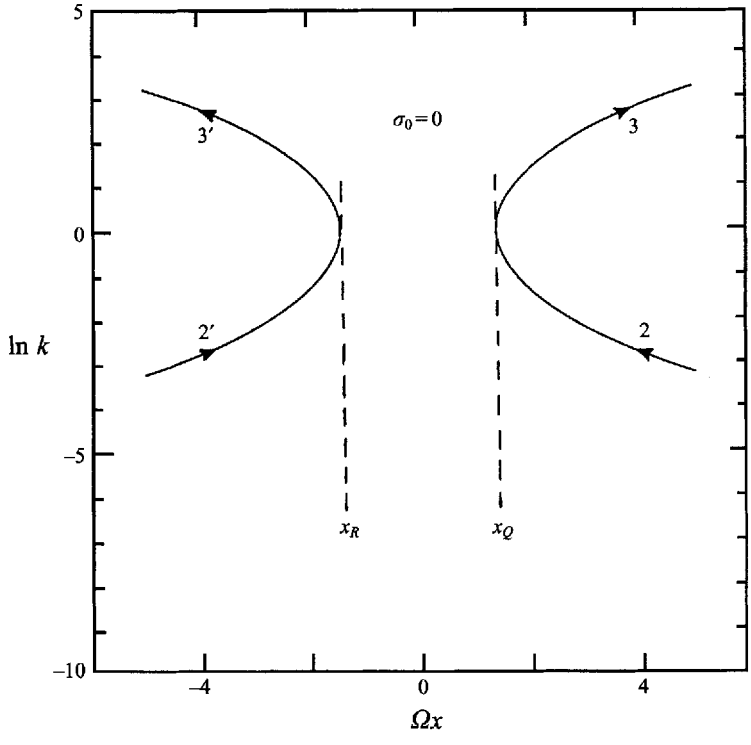

FIGURE 8. Wave systems in the (x,k)-plane when $\sigma_0 = 0$.

is made to somewhat exceed c_{min}. A two-dimensional object, such as a circular cylinder placed below the surface, will give rise to a train of gravity waves downstream. The waves will be stationary relative to the obstacle, so corresponding to the case $\sigma_0 = 0$. As the wave energy travels horizontally to the left, it will enter a region of decreasing surface current. It will be reflected near where the speed of the current equals 23 cm s^{-1}. Wave breaking at the caustic may possibly be avoided by adjusting the depth D of the cylinder to make the wave amplitude sufficiently small.

The distance of the caustic from the vertical barrier will depend on the depth of submergence H of the barrier. For small values of H the deceleration of the surface velocity will take place over a horizontal distance of the same order as H. As H increases we may expect the caustic to move further away from the barrier. In practice, the reflected train of capillary waves will shed a rectified vorticity (see Longuet-Higgins 1992) which will be convected backwards with the flow. This will create a turbulent circulation between the caustic and the vertical barrier OA, as indicated in figure 9. The phenomenon has been called a 'capillary bore' (Longuet-Higgins 1992). This however should not much affect the flow field outside the roller.

Because of the reduction in the potential flow towards the wall, we may expect the free surface to be slightly elevated above the undisturbed level. From Bernoulli's equation we expect the vertical displacement η to be given by

$$\eta = \frac{U^2}{2g} = \frac{\Omega^2 x^2}{2g}, \tag{6.1}$$

which has the form of a parabola. By hypothesis, η is small.

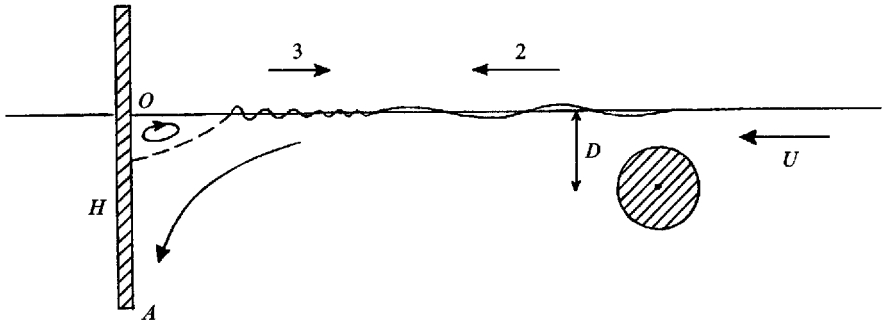

FIGURE 9. Arrangement for first experiment.

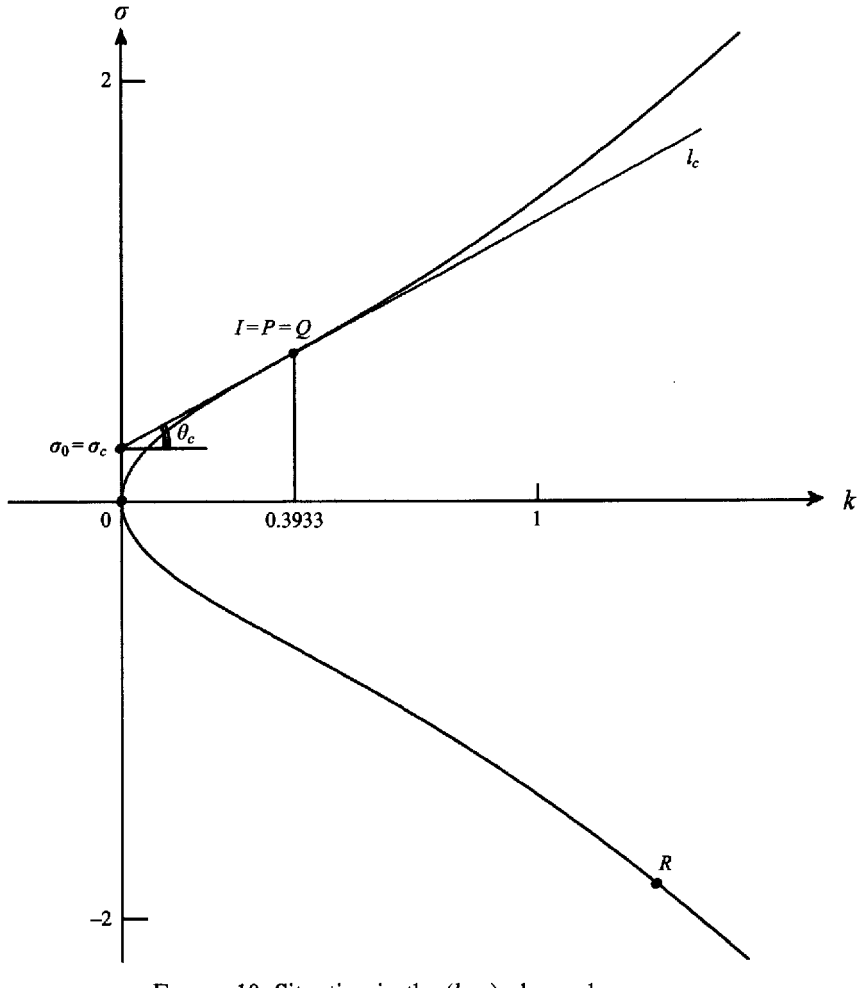

FIGURE 10. Situation in the (k, σ)-plane when $\sigma_0 = \sigma_c$.

If from the side of a ship moving at a slow speed (exceeding 23 cm s^{-1}) in still water – perhaps in a ship towing tank – a plane vertical barrier is inserted through the surface, then may expect to see a similar phenomenon; also just ahead of a moving ship with a blunt prow.

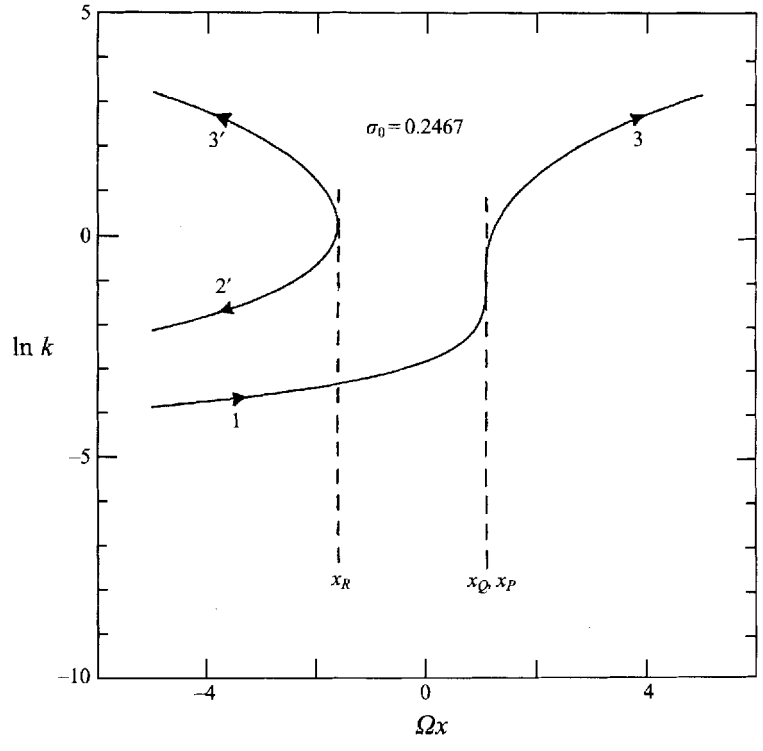

FIGURE 11. Wave systems in the (x,k)-plane when $\sigma_0 = \sigma_c$.

The formation of a capillary roller in this situation is suggested in figure 1(*b*) of Longuet-Higgins (1973), based on an observation made from a punt on the river Cam.

7. The critical case $\sigma_0 = \sigma_c$

The second interesting special case is when σ_0 is equal to the critical frequency σ_c; see figures 10 and 11. In figure 10, when $x > 0$, there is only one possible root k, and so in figure 11 there is only one possible wave train at each point. This special case is discussed by Trulsen & Mei (1993).

The value of σ_c is easily found by calculating the minimum positive group velocity:

$$c_g = \frac{\mathrm{d}\sigma}{\mathrm{d}k} = \frac{1+3k^2}{2(k+k^3)^{1/2}}. \tag{7.1}$$

This occurs when

$$k^2 = \frac{2}{\sqrt{3}} - 1 = 0.1547, \tag{7.2}$$

hence

$$k = 0.3933, \quad \sigma = \left(\frac{2}{\sqrt{3}}k\right)^{1/2} = 0.6739. \tag{7.3}$$

Also

$$c = 1.7134, \quad c_g = 1.0863. \tag{7.4}$$

Hence also

$$\sigma_0 = \sigma - kc_g = 0.2467. \tag{7.5}$$

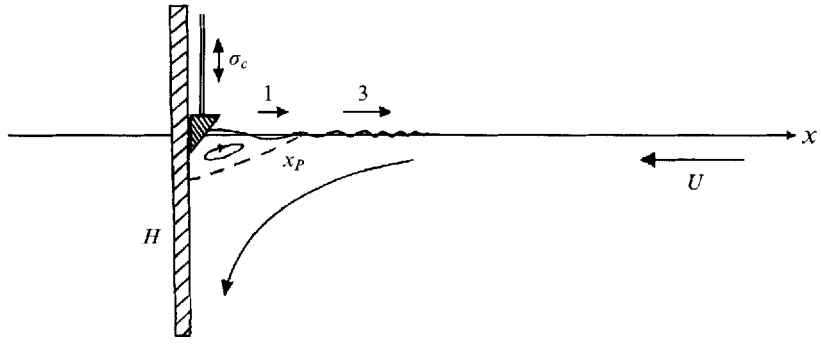

FIGURE 12. Arrangement for second experiment.

Thus the phase speed is greater and the group velocity less than the value $\sqrt{2}$ at $k = 1$. In this case x_P may be found from the fact that at the point of inflection $\Omega_x = \mathrm{d}\sigma/\mathrm{d}k$, hence

$$x_P = 1.0863\,\Omega^{-1}. \tag{7.6}$$

Thus x_P is closer to the origin O than in the previous example ($\sigma_0 = 0$).

From figure 11 we see that, in contrast to the previous case, the capillary wave (3) cannot be excited by a gravity wave (2) upstream of the caustic. On the other hand it can be excited by the gravity wave (1) from a point x anywhere to the left of x_P.

An experimental test of this conclusion might be conducted on the lines of the experiment in the previous Section, provided that the cylindrical obstacle is removed and replaced by a plunger at the left-hand wall, operating at a frequency $\omega = \sigma_c$; see figure 12. Although there may be some residual disturbance at the previous caustic, the caustic at the new value of x_P should be easily observable, since it lies to the left of its previous position.

8. Time-dependent wave trains

The general equation (2.4) for the energy E can easily be generalized to time-dependent wave trains by adding an extra term $\partial E/\partial t$ to the left-hand side (see Longuet-Higgins & Stewart 1964). This results in the addition of a term $\partial A/\partial t$ to (2.12). We confine attention here to the case when E and A are proportional to $\mathrm{e}^{\beta t}$, where β is independent of x and t. Then the conservation of phase (equation (2.3)) still applies. Since $\partial A/\partial t$ may be replaced everywhere by βA, equation (2.4) remains valid provided that the factor $4\nu k^2$ is replaced by $(4\nu k^2 + \beta)$. Then (3.5) becomes

$$B = \exp\left[\int \frac{4\nu k + \beta k^{-1}}{\partial U/\partial x}\,\mathrm{d}k\right] \tag{8.1}$$

and on substituting $\partial U/\partial x = -\Omega$ we obtain

$$B = B_0\, k^{\beta/\Omega}\, \mathrm{e}^{-2\nu k^2/\Omega}. \tag{8.2}$$

Here B_0 contains the time factor $\mathrm{e}^{\beta t}$. Hence we obtain a whole new class of solutions.

There is no obvious reason why such motions should not occur. However if $\beta > 0$ they would presumably grow until wave breaking or other nonlinear effects took place (the extra energy being supplied, as always, by the contracting current via the radiation stress). If $\beta < 0$ the waves would eventually die out. The chief reason for emphasizing the case $\beta = 0$ is that this is most likely to be observed in practice.

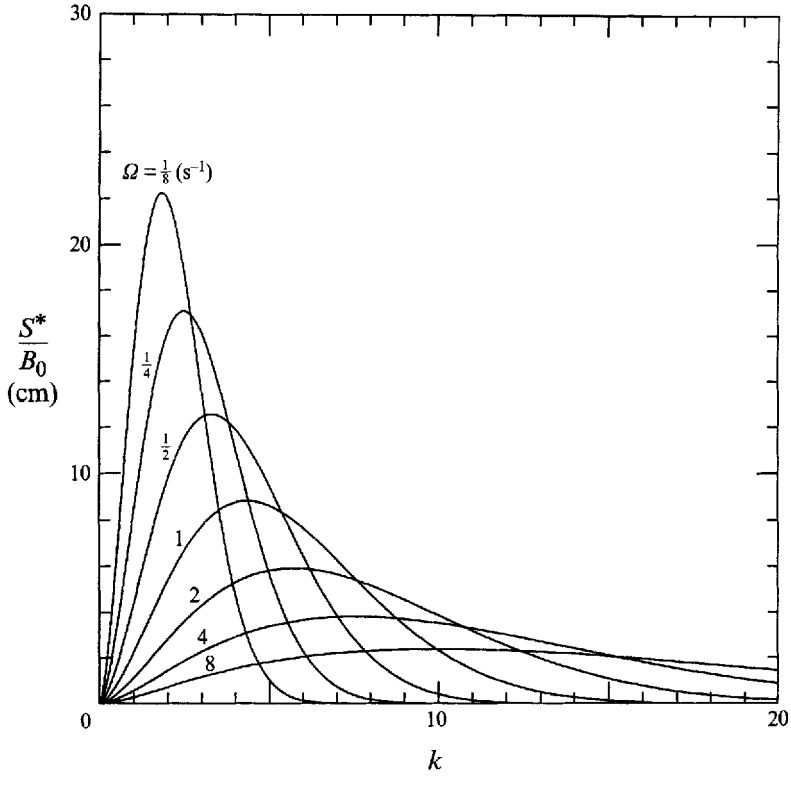

FIGURE 13. A plot of the slope spectrum $S^*(k)$ as given by equation (9.5) for various values of the strain rate Ω.

9. The energy spectrum

To find the overall energy spectrum of a wave train of varying amplitude and wavenumber we need to take account of the horizontal extent (Δx) of the surface over which the wave train has a wavenumber between k and $(k+\Delta k)$, say. This leads to the conclusion that the wavenumber spectrum $E^*(k)$ is related to the energy density E of §§2 and 3 by

$$E^* = E\left|\frac{\mathrm{d}x}{\mathrm{d}k}\right|. \tag{9.1}$$

But from (2.11) we have

$$\frac{\mathrm{d}k}{\mathrm{d}x} = -\frac{k\,\partial U/\partial x}{U+c_g} = \frac{k\Omega}{U+c_g}. \tag{9.2}$$

So combining (9.1) and (9.2) with (3.9) we obtain

$$E^* = \frac{\sigma B_0}{k\Omega}\mathrm{e}^{-2\nu k^2/\Omega}. \tag{9.3}$$

This very interesting result shows that the energy spectrum is independent of the parameter σ_0 (which enters the relation between x and k) and depends only on Ω and ν). Now the energy density E, as defined by (2.5), is the sum of contributions from the height spectrum and from the slope spectrum. These are represented by the two terms

a^2 and a^2k^2 in (2.5). If we wish to consider the slope spectrum S^* of the surface of itself, then we must multiply E^* by $k^2/(1+k^2)$. Thus from (9.3) we have

$$S^*(k) = \frac{B_0}{\Omega}\frac{\sigma k}{1+k^2}\mathrm{e}^{-2\nu k^2/\Omega}. \tag{9.4}$$

Since σ is given in terms of k by the dispersion relation (4.2) this becomes

$$S^*(k) = \frac{B_0}{\Omega}\frac{k^{3/2}}{(1+k^2)^{1/2}}\mathrm{e}^{-2\nu k^2/\Omega}. \tag{9.5}$$

In figure 13, $S^*(k)$ is plotted against k for representative values of the strain rate Ω.

Supposing for a moment that Ω were constant, equation (9.5) would appear to describe the wavenumber spectrum for surface waves near a typical downwelling point. Some caution is necessary because of the energy loss by wave breaking, particularly at a caustic.

The present work has been supported by the Office of Naval Research under Contract N00014-94-1-0008. A preliminary account was presented at the ONR Workshop on Free-surface Turbulence at Pasadena, CA, in March 1995.

REFERENCES

ALLEN, J. R. L. 1985 *Principles of Physical Sedimentology*. George Allen and Unwin.

BASOVICH, A. Y. & TALANOV, V. I. 1977 Transformation of short surface waves on inhomogeneous flows. *Izv. Akad. Nauk SSSR, Fiz. Atmos. i Okean.* **13**, 767–773.

BRETHERTON, F. P. & GARRETT, C. J. F. 1968 Wavetrains in homogeneous moving media. *Proc. R. Soc. Lond.* A **302**, 529–554.

GARRETT, C. J. F. 1967 The adiabatic invariant for wave propagation in a non-uniform moving medium. *Proc. R. Soc. Lond.* A **299**, 26–27.

KING, J. 1956 *British Columbia Handbook: Canada's West Coast*. Chico, California: Moon Publ.

LAMB, H. 1932 *Hydrodynamics*, 6th edn. Cambridge University Press.

LONGUET-HIGGINS, M. S. 1973 A model of flow separation at a free surface. *J. Fluid Mech.* **57**, 129–148.

LONGUET-HIGGINS, M. S. 1992 Capillary rollers and bores. *J. Fluid Mech.* **240**, 659–679.

LONGUET-HIGGINS, M. S. & STEWART, R. W. 1964 Radiation stresses in water waves; a physical discussion with applications. *Deep-Sea Res.* **11**, 529–562.

MATHES, G. H. 1947 Macroturbulence in natural stream flow. *Trans. Am. Geophys. Union* **28**, 255–265.

NEZU, I. & NAKAGAWA, H. 1993 *Turbulence in Open-Channel Flows*. Rotterdam: A. A. Balkema.

SHYU, J.-H. & PHILLIPS, O. M. 1990 The blockage of gravity and capillary waves by longer waves and currents. *J. Fluid Mech.* **217**, 115–141.

SMITH, R. 1975 The reflection of short gravity waves on a non-uniform current. *Math. Proc. Camb. Phil. Soc.* **78**, 517–528.

TRULSEN, K. & MEI, C. C. 1993 Double reflection of capillary–gravity waves by a non-uniform current. *J. Fluid Mech.* **251**, 239–271.